

Importance of interface sampling for extraordinary resistance effects in metal semiconductor hybrids

A. C. H. Rowe^{1,*} and S. A. Solin²¹*Laboratoire de Physique des Solides, Associé au CNRS, Bâtiment 510, Université Paris-Sud, 91405, Orsay, France*²*Department of Physics and Center for Materials Innovation, Washington University in St. Louis, 1 Brookings Drive, St. Louis, Missouri 63130 USA*

(Received 30 November 2004; revised manuscript received 9 February 2005; published 23 June 2005)

The magnitude of the extraordinary resistance change in metal semiconductor hybrid structures at 300 K under either magnetic field or tensile strain is known to depend strongly on geometry. In particular, there exists a range of optimal geometries for which the change in resistance under the external perturbation is maximized. Here we numerically solve Laplace's equation for circular hybrids in which the local resistivity is perturbed, and we show that within the range of optimal geometries (i) the metal-semiconductor interface is maximally sampled by the injected current and (ii) there is an observed crossover from semiconductor-like to metal-like conduction. Extraordinary resistance changes in metal semiconductor hybrids are thus considered to be interfacial effects.

DOI: 10.1103/PhysRevB.71.235323

PACS number(s): 72.80.Tm, 73.50.Dn, 73.50.Jt, 73.40.Mr

I. INTRODUCTION

Metal semiconductor hybrid structures have the potential to exhibit a large resistance change under a number of different external perturbations at 300 K. To date two such effects have been reported, the extraordinary magnetoresistance (EMR) (Ref. 1) and the extraordinary piezoconductance (EPC).² In the former, a perpendicular magnetic field induces a Hall angle between the current and electric field distribution in the hybrid, redirecting current away from the metal and leading to a large resistance increase. In the latter, a uniaxial tensile stress applied parallel to the metal semiconductor interface is thought to reduce the interface resistance, thereby redirecting current into the metal and reducing the measured resistance. Since the change in resistance can be more than an order of magnitude larger than that measured in the semiconductor alone, EXX (XX=MR or PC) has been proposed for a number of applications in which a sensitive measure of magnetic field^{3,4} or strain² is required.

EXX is first and foremost a geometrical effect, although its magnitude also depends (or is predicted to depend) on the material parameters (mobility, etc.) and the metal-semiconductor interface resistance.⁵ With respect to the geometry, efforts have already been made to maximize the EMR in rectangular hybrid structures for a specific application by changing the length-to-width ratio.⁶ In the most general terms "too little" metal, and the EXX tends toward that of the bulk semiconductor, "too much" metal and the EXX tends toward that of the bulk metal. At intermediate geometries when the amount of metal is "just right," the hybrid exhibits behavior not characteristic of either the bulk semiconducting or metal phases, and the EXX is maximized. Since these geometries appear to be at least approximately independent of whether the external perturbation is a magnetic field or a stress,² we ask what makes them special, i.e., what constitutes "too little" or "too much" metal, and what determines the optimal geometries? Here we show, via a nu-

merical solution of Laplace's equation for circular geometry hybrids, that the optimal geometries include that in which the interface is maximally sampled by the injected current, and that at this geometry a transition from semiconductor-like to metal-like conduction occurs. These results confirm that EXX effects in metal semiconductor hybrids are essentially interfacial phenomena.

II. DETAILS OF THE CALCULATION

Since it is of interest here to determine the special qualities of optimal hybrid geometries independent of the external perturbation, and since EXX effects are based on four-terminal resistance measurements, we calculate the so-called resistivity weighting function⁷ $f(r, \theta)$ for a range of circular planar hybrid geometries of uniform thickness. In a four-terminal resistance measurement a current is injected into the device via a pair of leads, and a voltage is measured elsewhere using a second pair of leads. The function $f(r, \theta)$ yields information on how the injected current samples each part of the device given the four lead locations. It is defined such that the effective overall resistivity of the device is given by

$$\rho_0^{\text{eff}} = \int \int \rho(r, \theta) f(r, \theta) r dr d\theta, \quad (1)$$

where $\rho(r, \theta)$ is the local resistivity and the integral is performed over the entire structure. In homogeneous devices $\rho(r, \theta) = \rho_0$ is a constant (material resistivity), whereas in hybrid structures component resistivities must also be accounted for. In particular, in circular hybrid geometries

$$\rho(r, \theta) = \rho_0(r, \theta) = \begin{cases} \rho_m & \text{if } r < r_m \\ \rho_s & \text{if } r_m < r < r_s \\ \infty & \text{if } r > r_s, \end{cases} \quad (2)$$

where ρ_m is the metal resistivity and ρ_s the semiconductor resistivity.¹² Here r_m and r_s are the metal and semiconductor

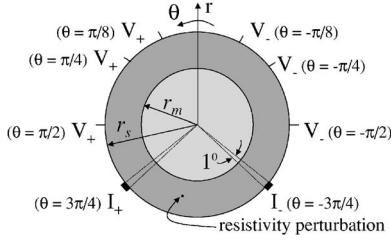


FIG. 1. Schematic of circular metal semiconductor hybrid structures considered here. The metallic (semiconducting) region is shown in light (dark) gray. The hybrid resistivity weighting function (HRWF) is calculated for pointlike voltage leads placed at $\theta = \pm\pi/8, \pm\pi/4$ and $\pm\pi/2$. Current leads of fixed width are located at $\theta = \pm 3\pi/4$. The small black dot indicated by the arrow represents the spatial extent of the resistivity perturbation Eq. (6), used to calculate the HRWF.

radii respectively, as shown in Fig. 1. In homogeneous structures it is possible to normalize $f(r, \theta)$ [i.e., $\iint f(r, \theta) r dr d\theta = 1$] so that for a structure uniformly sampled by the injected current $\rho_0^{\text{eff}} = \rho_0$, the material resistivity.⁷ In contrast, a normalization of $f(r, \theta)$ for hybrid structures is of limited utility since, even in the case of uniform current sampling, Eq. (1) results in a ρ_0^{eff} which corresponds neither to that of the metal or the semiconducting components of the hybrid. However, the inability to properly normalize $f(r, \theta)$ poses no problem since it is ratios of integrals of $f(r, \theta)$ that are of interest here (see below). In the following we utilize the expression hybrid resistivity weighting function (HRWF) for the non-normalized integrand of Eq. (1), $\rho(r, \theta)f(r, \theta)$ calculated for the circular hybrids.

The technique for calculating the HRWF is essentially the same as that previously applied to homogeneous Hall bar and van der Pauw structures.⁷ Ideally, a pointlike perturbation at (r_0, θ_0) in the local resistivity is introduced in the following form:

$$\rho(r, \theta) = \rho_0(r, \theta) + \epsilon \rho_0^{\text{eff}} \frac{1}{r} \delta(r - r_0) \delta(\theta - \theta_0). \quad (3)$$

Here the factor $1/r$ is introduced to properly normalize the δ functions in cylindrical polar coordinates. When this expression is substituted into Eq. (1) in order to calculate a perturbed effective resistivity $\rho_{\text{pert}}^{\text{eff}}$, we find that

$$f(r_0, \theta_0) = \frac{1}{\epsilon} \frac{(\rho_{\text{pert}}^{\text{eff}} - \rho_0^{\text{eff}})}{\rho_0^{\text{eff}}}. \quad (4)$$

In practice it is a voltage difference proportional to the resistivity that is calculated, so we write

$$f(r_0, \theta_0) = \frac{1}{\epsilon} \frac{\Delta V}{V_0}, \quad (5)$$

where $\Delta V = V_{\text{pert}} - V_0$ and V_0 (V_{pert}) is the voltage calculated between the voltage leads in the absence (presence) of the perturbation, Eq. (3).

A. Calculation of V_0

In order to calculate V_0 the current and electric field distribution in the hybrid must be found. In steady state at 300 K, the problem reduces to a solution of Laplace's equation, $\nabla^2 V = 0$ for the scalar electric potential across the hybrid. In circular geometry hybrids with symmetrically placed leads an analytic solution exists,^{8,9} but for nonsymmetric or rectangular geometry hybrids numerical methods such as a finite element analyses (FEA) must be employed.¹⁰ In this article both symmetric and nonsymmetric geometries will be considered, so we utilize FEA techniques. The following external boundary conditions are imposed for all calculations: (1) Constant normal current at the two current leads $\mathbf{J}_r = \mathbf{J}_0$ and (2) Zero normal current flow for the remaining external boundaries $\mathbf{J}_r = \mathbf{0}$. Furthermore, the discontinuity in ρ at $r = r_m$ is accounted for by an internal boundary condition: (3) Continuity of the normal component of the current at the metal semiconductor interface.

In all results presented here the current leads have a finite width and subtend an angle of 1° at the center of the hybrid, whereas the voltage leads have zero width. The absence of finite width voltage leads does not significantly affect the results and facilitates parallel calculations of the HRWF for different voltage lead positions [$\theta = \pm\pi/8, \pm\pi/4$ (the symmetric case) and $\pm\pi/2$]. This is useful to separate the role of voltage lead position and $\alpha = r_m/r_s$ in the determination of the optimal geometry. The current lead positions are fixed at $\theta = \pm 3\pi/4$. These details are shown in Fig. 1. It should also be noted that a fixed value $r_s = 1$ is chosen (units are arbitrary) and r_m is varied.

B. Calculation of ΔV

FEA techniques are also useful when considering the effect of a local inhomogeneity, for example in the magnetic field¹¹ or (as in this case) in the resistivity.⁷ In a FEA calculation, it is not possible to introduce local inhomogeneities of the form given in Eq. (3). Rather a differentiable but arbitrary function which approximates Eq. (3) should be utilized. For the purposes of the calculation performed here, the resistivity perturbation has the arbitrary super Gaussian form

$$h_0 \exp\{-[r^2 + r_0^2 - 2rr_0 \cos(\theta - \theta_0)]/(w_0/2)^2\}^{200}, \quad (6)$$

where $h_0 = 1 \times 10^{-5} \Omega \text{ m}$ and $w_0 = 0.03$. The amplitude h_0 is chosen to be small enough that the voltage response is in the linear regime. This function yields a flat-topped resistivity perturbation with a size indicated by the black dot in Fig. 1, and fixes the spatial resolution of the calculations at $\alpha = \pm 0.015$. Both r_0 and θ_0 are varied stepwise over the entire hybrid in order to build up a grayscale image of the HRWF for a given α as shown in Figs. 2, 5, and 7. The equation of motion must now also include a forcing term in order to properly account for the local resistivity perturbation⁷

$$\nabla^2 V = \nabla \rho \nabla V / \rho. \quad (7)$$

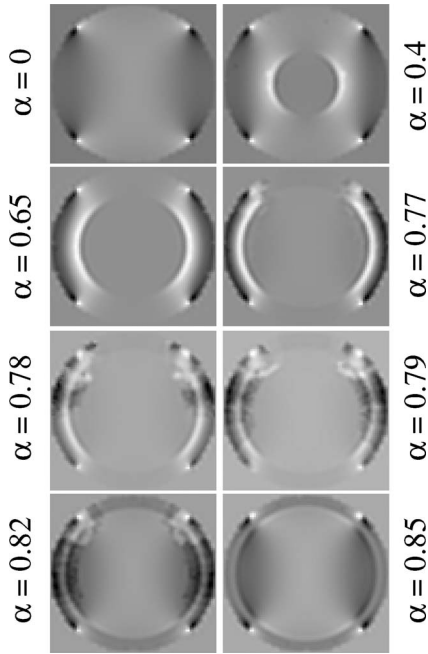


FIG. 2. Grayscale images of the HRWF for a symmetric hybrid. From top left to bottom right, $\alpha=0, 0.4, 0.65, 0.77, 0.78, 0.79, 0.82,$ and 0.85 . Lighter shaded regions are more strongly sampled by the injected current. It is noted that for $\alpha < 0.78$ the metal is only weakly sampled and the metal-semiconductor interface region is most strongly sampled (in white). For $\alpha > 0.78$ the metal begins to be sampled more strongly, and the importance of the interface region dies off.

III. RESULTS AND DISCUSSION

A. Voltage leads at $\theta = \pm \pi/4$

Figure 2 shows the HRWF for a variety of geometries in a symmetric circular hybrid. In each of these images white (black) areas are strongly (weakly) sampled by the injected current. Thus we see that at small values of α (< 0.78) the metallic part of the hybrid plays a very little role in determining the electrical properties. Rather it is mainly a region localized near the metal-semiconductor interface which dominates the electrical properties (plus a small, relatively negligible surface area adjacent to the current and voltage leads). It is also visually apparent that with increasing α the relative importance of the interface region becomes stronger up to and including $\alpha=0.77$. As α is further increased, the metal begins to play a role in the overall resistivity, and the relative importance of the interface region diminishes. At the largest value of α shown in Fig. 2, it is clear the the metallic region is a very important, if not the dominant part of the hybrid for the purposes of a four-terminal resistance measurement.

These qualitative observations can be better quantified by a calculation of $\iint \rho(r, \theta) f(r, \theta) r d\theta dr$ over the appropriate part of the hybrid. In the following, \mathbf{M} is this integral performed over the metallic region, \mathbf{S} over the semiconducting region, and \mathbf{I} over the interface region (defined as $r_m < r < r_m + w_0$). A measure of the relative importance of the interface region is then given by $\mathbf{I}/(\mathbf{M}+\mathbf{S})$. Similarly, \mathbf{M}/\mathbf{S}

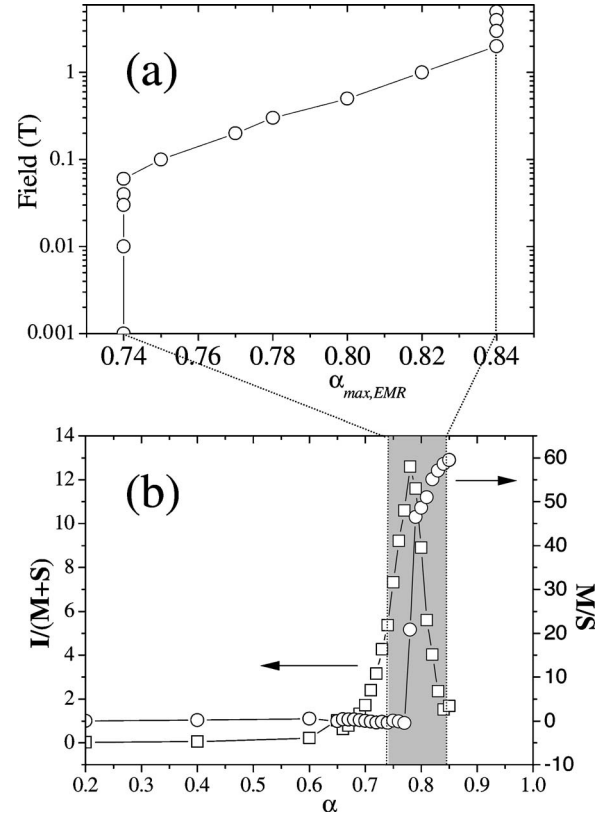


FIG. 3. (a) Variation in the optimal geometry ($\alpha_{\max,EMR}$) with field due to variation in the Hall angle for a symmetric hybrid. $\alpha_{\max,EMR}$ varies from 0.74 at low fields to 0.84 at high fields. This range is shown as the gray region in (b). (b) $\mathbf{I}/(\mathbf{M}+\mathbf{S})$ (squares) and \mathbf{M}/\mathbf{S} (circles) calculated as a function of α from the HRWF. The peak in the former at $\alpha=0.78$, corresponding to a maximum sampling of the interface region by the injected current lies in the optimal range of EMR geometries (gray region). The change from semiconducting behavior ($\mathbf{M}/\mathbf{S} < 1$) to metallic behavior ($\mathbf{M}/\mathbf{S} > 1$) also occurs at $\alpha=0.78$.

is a measure of the character of the hybrid resistivity $\mathbf{M}/\mathbf{S} < 1$ corresponding to a semiconductor-like hybrid, and $\mathbf{M}/\mathbf{S} > 1$ corresponding to a metallic-like hybrid). For the symmetric hybrid, these two quantities are shown in Fig. 3.

A peak in $\mathbf{I}/(\mathbf{M}+\mathbf{S})$ for $\alpha=0.78$ indicates that at this geometry, the metal-semiconductor interface has its greatest influence on a four-terminal resistance measurement of the hybrid. It is also at this geometry that the hybrid switches from metallike to semiconductinglike behavior. In this (symmetric) case, the latter result is experimentally verified by measuring the resistance versus temperature curves for a range of symmetric circular hybrids¹³ as shown in Fig. 4. Each hybrid was measured using standard lock-in techniques at temperatures ranging from 300 to 1.5 K. A clear demarcation between semiconducting and metallic behavior is seen around $\alpha=12/16$ (0.75) where the resistance is approximately independent of temperature. For $\alpha < (>) 12/16$ the resistance increases (decreases) with decreasing temperature, typical of semiconducting (metallic) behavior. Within the limits of the experimentally available values of α (the next greatest value being $13/16=0.825$) this is in agreement with the calculation.

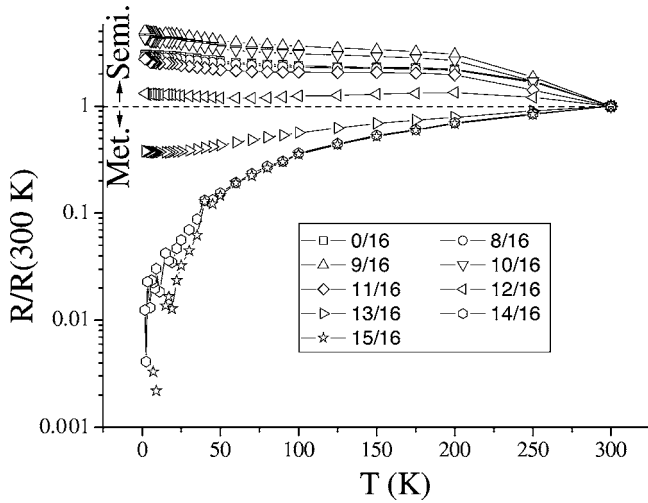


FIG. 4. Measured four-terminal resistance of circular symmetric hybrids as a function of temperature and α , normalized to the measured resistance at 300 K. The switch between semiconducting (Semi.) and metallic (Met.) behavior occurs for $12/16 < \alpha < 13/16$, in agreement with the ratio M/S calculated from the HRWF.

The optimal EMR geometry depends weakly upon the Hall angle and thus varies with magnetic field as shown in Fig. 3(a), and this range of geometries is represented as a gray region in Fig. 3(b). The optimal geometry for interface sampling falls in this range for the symmetric hybrid. Based on the proposed mechanism for the EPC effect (i.e., a reduction in the metal semiconductor interface resistance with stress)² it is self-evident that the maximum EPC will occur at the optimal geometry for interface sampling.

A change in current and/or voltage lead position will also modify the optimal value of α for interface sampling. It is therefore of interest to investigate whether the optimal EMR geometries always include that in which the metal-semiconductor interface is maximally sampled regardless of lead position. To this end we consider two further hybrid geometries in which the voltage lead position is varied. It is expected that a change in current lead position will yield qualitatively similar results.

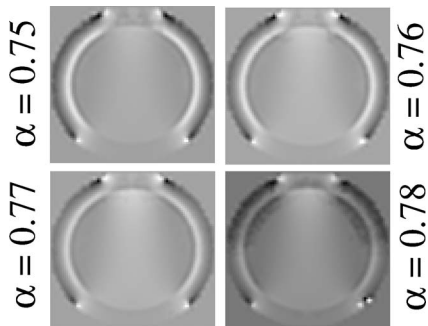


FIG. 5. Grayscale images of the HRWF for voltage leads placed at $\theta = \pm \pi/8$. Four images are shown near the optimal geometry for interface sampling ($\alpha = 0.75$), which also corresponds to a switch from semiconducting to metalliclike behavior. Sampling of the metal is evident at $\alpha = 0.78$.

B. Voltage leads at $\theta = \pm \pi/8$

Grayscale images of the HRWF near the optimal EMR geometries for a hybrid with voltage leads placed at $\theta = \pm \pi/8$ are shown in Fig. 5. As in the case of the symmetric hybrid already considered, the interface region is most strongly sampled (i.e., in white) by the injected current. Similarly, in the image presented for $\alpha = 0.78$ there are two notable characteristics, namely, (i) the metal region clearly starts to be sampled by the injected current and (ii) the sampling of the interface region, especially near the voltage leads, is clearly reduced. This behavior is qualitatively similar to the case of the symmetric hybrid.

In fact a calculation of the ratios $I/(M+S)$ and M/S shows, respectively, that maximal interface sampling occurs at $\alpha = 0.75$ and that this corresponds to a switch between semiconducting and metallic behavior [see Fig. 6(b)]. This geometry lies in the range of optimal geometries for EMR [see Fig. 6(a)] represented in gray in Fig. 6(b). It will be noted that S , and hence the ratio M/S , is negative for

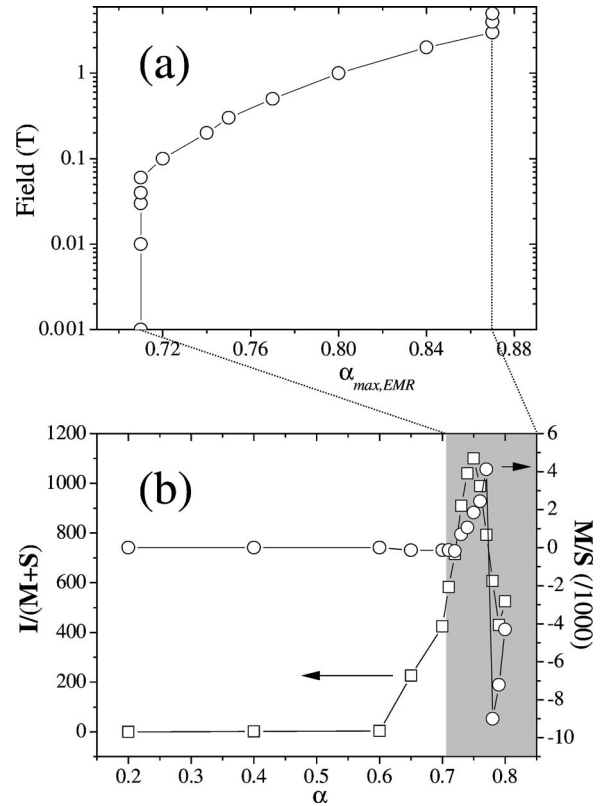


FIG. 6. (a) Variation in the optimal geometry ($\alpha_{max,EMR}$) with field due to variation in the Hall angle for a hybrid with voltage leads placed at $\theta = \pm \pi/8$. $\alpha_{max,EMR}$ varies from 0.71 at low fields to 0.87 at high fields. This range is shown as the gray region in (b). (b) $I/(M+S)$ (squares) and M/S (circles) calculated as a function of α from the HRWF. The peak in the former at $\alpha = 0.75$, corresponding to a maximum sampling of the interface region by the injected current falls in the optimal range of EMR geometries (gray region). The change from semiconducting behavior ($M/S < 1$) to metallic behavior ($M/S > 1$) also occurs at $\alpha = 0.75$. Note that for $\alpha > 0.77$ the contribution from the semiconductor is negative (i.e., it reduces the overall resistance), and thus M/S is also negative.

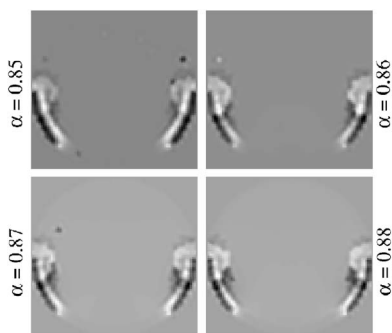


FIG. 7. Grayscale images of the HRWF for voltage leads placed at $\theta = \pm \pi/2$. Four images are shown near the optimal geometry for interface sampling, and the switch from semiconducting to metallic behavior.

$\alpha > 0.77$. The main negative contribution to \mathbf{S} arises near the edge of the hybrid close to the voltage leads as can be seen from the black areas in Fig. 5, $\alpha = 0.78$. This is a somewhat counterintuitive result since it implies that the presence of the semiconductor actually *reduces* the overall resistance. However, the absolute contribution of the metal is greater than that of the semiconductor, and so the overall resistance is positive as required.

C. Voltage leads at $\theta = \pm \pi/2$

A qualitatively similar result is obtained for voltage leads placed at $\theta = \pm \pi/2$, although the onset of current sampling of the metal is less visually evident than the previous two cases

(see Fig. 7). It remains evident that the interface region is of greatest importance for a resistance measurement. Within the spatial resolution of the calculation ($w_0/2$), the HRWF shows that the optimal geometry for interface sampling corresponds to that for the switch from semiconducting to metallic behavior ($\alpha = 0.87$ and $\alpha = 0.86$, respectively). This geometry again falls within the range of geometries optimal for EMR ($0.84 < \alpha < 0.92$).

IV. CONCLUSION

Based on calculations of the HRWF for a range of circular metal-semiconductor hybrid geometries it has been shown that maximal EXX is obtained in geometries where the sampling of the metal-semiconductor interface by the injected current is maximized. The latter geometry also corresponds to a measured change from semiconducting-like to a metallic-like behavior in the four-terminal hybrid resistance. Although the absolute optimal value of α depends on the location of the current and voltage leads, the calculations indicate that the above conclusions hold regardless of lead location. Thus although the magnitude of the EXX depends on a number of parameters, it is essentially an interface phenomenon. As a general “rule-of-thumb” therefore, maximizing EXX for applications should be achievable by designing hybrids in which the metal-semiconductor interface is maximally sampled by the injected current.

ACKNOWLEDGMENTS

A.C.H.R. acknowledges H. Bouchiat for useful discussions. S.A.S. is supported by the U.S. National Science Foundation under Grant No. ECS0329347.

*Permanent address: Laboratoire de physique de la matière condensée, École Polytechnique, 91128 Palaiseau Cedex, France.

¹S. A. Solin, D. R. Hines, T. Thio, and J. Heremans, *Science* **289**, 1530 (2000).

²A. C. H. Rowe, D. R. Hines, and S. A. Solin, *Appl. Phys. Lett.* **83**, 1160 (2003).

³S. A. Solin, D. R. Hines, A. C. H. Rowe, J. S. Tsai, Y. A. Pashkin, S. J. Chung, N. Goel, and M. B. Santos, *Appl. Phys. Lett.* **80**, 4012 (2002).

⁴C. H. Möller, O. Kronenworth, C. Heyn, and D. Grundler, *Appl. Phys. Lett.* **84**, 3343 (2004).

⁵M. Holz, O. Kronenworth, and D. Grundler, *Phys. Rev. B* **67**, 195312 (2003).

⁶M. Holz, O. Kronenworth, and D. Grundler, *Appl. Phys. Lett.* **83**, 3344 (2003).

⁷D. W. Koon and C. J. Knickerbocker, *Rev. Sci. Instrum.* **63**, 207

(1992).

⁸T. Zhou, S. A. Solin, and D. R. Hines, *J. Magn. Magn. Mater.* **226**, 1976 (2001).

⁹D. Poplavskyy, *J. Magn. Magn. Mater.* **267**, 406 (2003).

¹⁰J. Moussa, L. R. Ram-Mohan, J. Sullivan, T. Zhou, D. R. Hines, and S. A. Solin, *Phys. Rev. B* **64**, 184410 (2001).

¹¹J. Moussa, L. R. Ram-Mohan, A. C. H. Rowe, and S. A. Solin, *J. Appl. Phys.* **94**, 1110 (2003).

¹²In the calculation presented here $\rho_m = 2.2 \times 10^{-8} \Omega \text{m}$, the resistivity of Au, and $\rho_s = 5.4 \times 10^{-5} \Omega \text{m}$, the resistivity of Te-doped ($n = 2.55 \times 10^{22} \text{m}^{-3}$) InSb.

¹³The symmetric structures used in these measurements were those fabricated for the original report of EMR, where a complete description of sample preparation and measurement can be found (see Ref. 1).